

# Spectroscopic Characterization of Solvent-Mediated Folding in Dicarboxylate Dianions\*\*

Torsten Wende, Marius Wanko, Ling Jiang, Gerard Meijer, Knut R. Asmis,\* and Angel Rubio\*

Dicarboxylate salts play an important role in many areas of science, including atmospheric chemistry, biochemistry, and synthetic chemistry. For example, they are used as antitumor drugs<sup>[1]</sup> and as building blocks for metal–organic framework materials,<sup>[2]</sup> and they are found in aerosol particles comprising photochemical smog.<sup>[3]</sup> Isolated dicarboxylate dianions are stable in the gas phase and serve as model systems for multiply charged anions.<sup>[4,5]</sup> The presence of two charge centers separated by a hydrophobic, aliphatic chain also makes them ideal for studying charge screening and solvent-mediated effects.<sup>[6]</sup> Herein, we use gas-phase infrared (IR) spectroscopy of the microhydrated suberate dianion ( $\text{SA}^{2-}$ ,  $^-\text{OOC}(\text{CH}_2)_6\text{COO}^-$ ) together with quantum chemical calculations to establish relationships between conformational changes and spectroscopic features. We then analyze how hydration can drive a conformational transition in a dianion and what role the hydrogen-bonded network plays.

Gas-phase action spectroscopy<sup>[7]</sup> is a powerful tool to study the effects of microhydration on the conformation of dicarboxylate dianions, adding one water molecule at a time. Anion photoelectron spectra in combination with quantum chemical calculations<sup>[6,8,9]</sup> found a delicate dependence of the conformation of the dicarboxylate dianion on the degree of hydration, the aliphatic chain length, and the temperature. More detailed insight into the folding mechanism requires structural information, which is challenging to extract from the photoelectron data. IR photodissociation (IRPD) spectroscopy combined with high-level quantum chemical calculations on microhydrated anions<sup>[10–12]</sup> is able to supply this information and thus leads to a considerably more detailed

understanding of this hydration-mediated folding process at the molecular level.

Recent IRPD spectra of  $\text{SA}^{2-}$  and its monohydrate  $\text{SA}^{2-}\cdot\text{H}_2\text{O}$  revealed how the addition of a water molecule affects the spectroscopic signature of the dianion.<sup>[13]</sup> The water molecule binds to one of the carboxylate groups of the quasi-linear dianion, thus causing characteristic shifts of the intense IR-active carboxylate stretching bands. The two symmetric ( $\nu_s$ ) and two antisymmetric ( $\nu_a$ ) carboxylate stretching modes in  $\text{SA}^{2-}$  are in each case quasi-degenerate, because each pair of modes is weakly coupled as a result of the large distance between the carboxylate groups. Addition of a single water molecule lifts this degeneracy and leads to a characteristic splitting of both bands (compare the spectra for  $n=0$  and  $n=1$  in Figure 1).

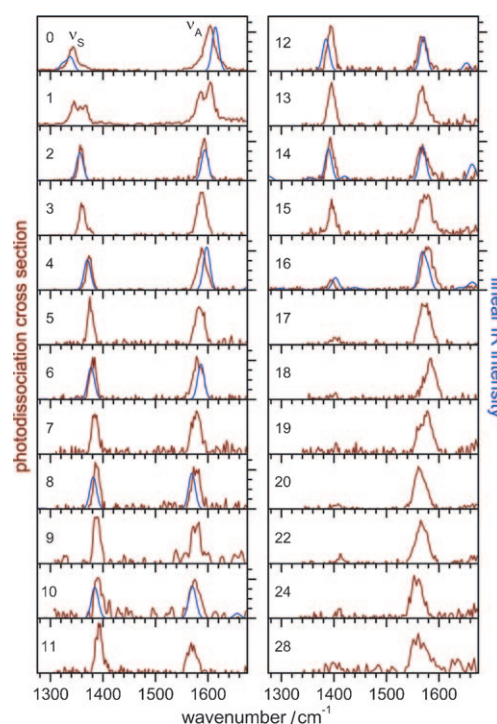


**Figure 1.** Experimental IRPD spectra (red) of  $\text{SA}^{2-}(\text{H}_2\text{O})_n$  clusters with  $n=0$ –28 and simulated linear IR absorption spectra (blue) for  $n=0, 2, \dots, 16$  in the region of the  $\nu_s$  and  $\nu_a$  carboxylate stretching modes. The spectra for  $n=0$  and  $n=1$  are taken from Ref. [13].

We measured IRPD spectra of  $\text{SA}^{2-}(\text{H}_2\text{O})_n$  up to  $n=28$  (Figure 1). The ions are produced in an electrospray source at room temperature and then cooled to cryogenic temperatures by many collisions with a buffer gas prior to irradiation with intense and tunable IR radiation. As a probe, we focus on the

[\*] T. Wende, L. Jiang, G. Meijer, K. R. Asmis  
 Fritz-Haber-Institut der Max-Planck-Gesellschaft  
 Faradayweg 4–6, 14195 Berlin (Germany)  
 E-mail: asmis@fhi-berlin.mpg.de

M. Wanko, A. Rubio  
 Nano-Bio Spectroscopy Group and ETSF Scientific Development  
 Centre, Departamento de Física de Materiales, Universidad del País  
 Vasco, Centro de Física de Materiales CSIC-UPV/EHU-MPC and  
 DIPC  
 Av. Tolosa 72, 20018 San Sebastián (Spain)  
 E-mail: angel.rubio@ehu.es

[\*\*] We thank the Stichting voor Fundamenteel Onderzoek der Materie (FOM) for beamtime and the staff for support and assistance. This research is funded by the European Community's Seventh Framework Programme (FP7/2007-2013, grant nr. 226716), the Spanish MEC (FIS2007-65702-C02-01), the "Grupos Consolidados UPV/EHU del Gobierno Vasco" (IT-319-07), and CIC NanoGUNE (grant no. CSD2006-53). L.J. thanks the Alexander von Humboldt Foundation for a postdoctoral scholarship.

Supporting information for this article is available on the WWW under <http://dx.doi.org/10.1002/anie.201006485>.

carboxylate stretching modes, which lie in the spectral region 1300–1650  $\text{cm}^{-1}$ . The photodissociation cross section is plotted as a function of the photon energy. Inspection of the sequential shift of the IRPD bands as a function of the number of water molecules in the cluster (Figure 2, left)

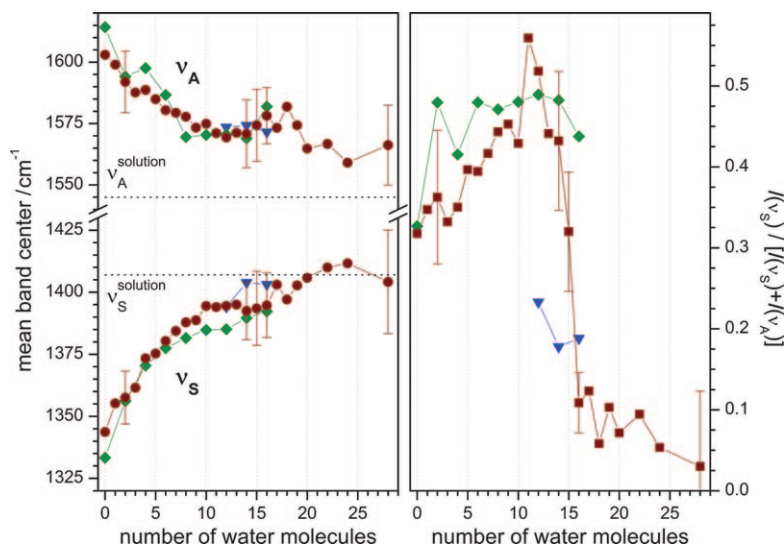


**Figure 2.** Center of the  $\nu_s$  and  $\nu_a$  bands (left) and intensity ratio  $I(\nu_s)/[I(\nu_s)+I(\nu_a)]$  (right) for microhydrated  $\text{SA}^{2-}(\text{H}_2\text{O})_n$  clusters as a function of  $n$ . Experimental values (red circles) as well as computed values for linear (green diamonds) and folded (blue triangles) geometries are shown. Error bars indicate the standard deviation (Table S1 in the Supporting Information). Lines connecting the symbols are drawn to guide the eye. Dotted horizontal lines indicate absorption frequencies in solution.

reveals that the  $\nu_a$  band shifts to lower (1603→1566  $\text{cm}^{-1}$ ) and the  $\nu_s$  band to higher energies (1344→1404  $\text{cm}^{-1}$ ) with an increasing number of water molecules. This sequential shift is nearly monotonic and decreases gradually with increasing values of  $n$ . The frequencies of aliphatic dicarboxylate dianions in bulk solution, for example, pimelate ( $\nu_a = 1545 \text{ cm}^{-1}$ ,  $\nu_s = 1407 \text{ cm}^{-1}$ ),<sup>[14]</sup> are reached for  $\nu_s$  but not for  $\nu_a$  (Figure 2), thus suggesting that  $\nu_a$  is more sensitive to long-range solvent effects than  $\nu_s$ .

While the sequential band shifts are rather regular in nature, the behavior of the band intensities shows a pronounced size dependence. This effect is best seen in Figure 1 for the IRPD spectra of  $n \geq 14$ , where the intensity of the  $\nu_s$  band drops significantly at  $n = 16$  and remains low throughout the spectra of the larger clusters. A more quantitative analysis, involving the normalized intensity  $I(\nu_s)/[I(\nu_s)+I(\nu_a)]$ , is plotted in Figure 2 (right). The ratio increases from 0.32 at  $n = 0$  to above 0.50 at  $n = 11$ , after which it drops down to 0.11 at  $n = 16$  and remains small for all larger water clusters.

To elucidate the origin of this behavior, we determined the minimum-energy structures for both linear and folded geometries for even values of  $n$  up to  $n = 16$  (see the Supporting Information) and derived IR spectra (Figure 1, blue traces) from calculated harmonic vibrational frequencies and IR intensities. All simulated IR spectra of the folded geometries show a strong reduction in intensity of the IR-active  $\nu_s$  mode, whereas the  $\nu_a$  mode remains strong and

decoupled, like in the linear configuration (Figure 2, right). As shown in Figure S3 in the Supporting Information, this trend is independent of the particular structure of the water cluster. Note that minor deviations between the experimental IRPD cross sections and the calculated linear absorption spectra are expected, owing to the multiple-photon nature of the absorption process.<sup>[15]</sup>

The IR intensity of a vibrational mode is proportional to the square of the change in dipole moment  $\mu$  when the geometry is displaced along the corresponding normal coordinate ( $|d\mu/dQ|^2$ ). Displacement along the  $\nu_a$  mode causes a strong charge transfer (CT) between the two carboxylate oxygen atoms, as it breaks the symmetry of the resonance structure. Owing to the local character of this CT, it is independent of the geometry of the polyethylene chain and is hence unaffected by the folding. This situation is in contrast to excitation of  $\nu_s$ , where a smaller but long-range CT between the carboxylate moiety and the chain occurs, which is sensitive to changes in dihedral angles upon folding (Figure 3). Furthermore, this CT between the hydrophobic and hydrophilic moieties responds strongly to hydration, and it will be affected by the mutual polarization of the carboxylates. Apart from the static polarization, we also find a subtle resonance effect arising from the interaction of the fluctuating dipoles induced by excitation of  $\nu_s$  (Figure 3). We isolated this

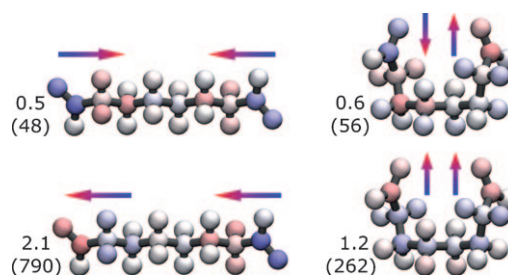


**Figure 3.** Natural population analysis (NPA) difference charges induced by displacement along  $\nu_s$  modes for linear (left) and folded (right)  $n = 12$  clusters (water molecules not shown). Blue: electron-rich, red: electron-poor, gray: neutral.  $|d\mu/dQ|$  is given in  $10^{-2}$  a.u., intensity  $I$  (in parentheses) in  $\text{km mol}^{-1}$ .

effect for  $n = 12$  by calculating the spectrum with isotopically labeled oxygen atoms ( $^{18}\text{O}$ ) on one of the two carboxylate groups to decouple the two resonating COO stretching modes. As a result, the value of  $I(\nu_s)$  decreases for the linear structure and increases for the folded structure (Table S4 in the Supporting Information).

While the relationship between cluster size and folding is clearly established, the investigation of the folding mechanism in the low-temperature regime remains challenging. Both experiments and classical molecular dynamics (MD) simulations face the problem that a thermodynamic equilib-

rium between linear and folded structures cannot be obtained at cryogenic temperatures.<sup>[6,9]</sup> As suggested by Wang et al.,<sup>[6,9]</sup> this situation is due to a folding barrier that originates from the long-range Coulomb repulsion between the charged moieties, which is counteracted by additional hydrogen bonds that form in the folded structures (Table S2 in the Supporting Information). Our MD simulations support this model in several respects. Even at 230 K, we find low folding and unfolding rates. A typical folding event in the MD trajectory (see the Supporting Information for a movie for  $n = 16$ ) shows a three-step process. First,  $SA^{2-}$  rests in an intermediate state in which the separation between the carboxylates is reduced by isomerization of two C–C bonds, that is, the outermost C–C–C–C dihedral angles assume a value of approximately  $\pm 65^\circ$ . Then, the first hydrogen bond forms between the two separate water clusters, and finally, the formation of additional hydrogen bonds allows for isomerization of a third C–C bond, which defines the folded state (Table S3).

For the  $n = 14$  complex, Wang et al. have shown that linear and folded structures are in equilibrium at 108 K.<sup>[6,9]</sup> While at higher temperatures the linear form is more stable, a negative folding energy  $E_f$  of  $-1.7 \text{ kcal mol}^{-1}$  was extrapolated for the 0 K limit. This information can be used to assess quantum chemical calculations on the minimum-energy structures. To investigate the folding energetics, we performed CEPA/1 calculations (with ZPVE correction from PBE). Compared with the experimental estimate for  $n = 14$ , the method underestimates  $E_f$  by 4.4–4.6 and 1.1–1.3  $\text{kcal mol}^{-1}$  when double- $\zeta$  and triple- $\zeta$  basis sets, respectively, are used. Assuming the same error for  $n = 12$ , the linear structure would be more stable by merely 1–2  $\text{kcal mol}^{-1}$  at 0 K (Table 1).

**Table 1:** Decomposition of the folding energy  $E_f$  [ $\text{kcal mol}^{-1}$ ].<sup>[a]</sup>

$n$	$E_{\text{Coul}}^{\text{[b]}}$	SA	Water	$SA^{2-}$ –water	ZPVE	$E_f$
12	26.5	23.0	5.6	–33.7	2.7	–2.4
14	38.7	31.1	24.0	–63.0	1.8	–6.1
16	23.2	18.6	3.5	–31.5	2.6	–6.8

[a] CEPA/1 calculations (aug-cc-pVDZ basis set and MP2/TZVP geometries); ZPVE from PBE/aug-cc-pVDZ. [b] Bare Coulomb interaction of the  $COO^-$  fragments (including intermolecular CT).

A decomposition of  $E_f$  based on fragment calculations is shown in Table 1. The Coulomb repulsion between the carboxylates increases by 20–40  $\text{kcal mol}^{-1}$  upon folding, which essentially constitutes the folding energy of the bare  $SA^{2-}$  ion when the water molecules in the calculation are omitted. The rise in energy is compensated by the interaction between the  $SA^{2-}$  ion and the water cluster and reflected in the formation of additional hydrogen bonds, mostly between the dianion and the water molecules (Table S2 in the Supporting Information). Surprisingly, the water–water interaction does not contribute to folding, as the energy of the water cluster is not lowered by folding when  $SA^{2-}$  is omitted in the calculation.

The present results allow us to draw the following conclusions:

- 1) The intensity of the IR-active symmetric carboxylate stretching mode represents a sensitive probe to distinguish between linear and folded dicarboxylate dianions, because this mode strongly responds to the coupling between the carboxylate group and the aliphatic chain.
- 2) In contrast, the frequencies of the carboxylate stretching modes are more sensitive to the local hydrogen-bonding network. Higher resolution techniques can exploit this effect to determine more detailed structural information.
- 3) The stabilization of the folded dianion structures is essentially due to the formation of additional solute–solvent (rather than solvent–solvent) hydrogen bonds. Therefore, the folded structures should also persist in much larger microhydrated clusters at sufficiently low temperature.

The present findings should have important implications for probing the structure of dicarboxylic acids and their ions in the condensed phase, as well as for remote sensing applications used, for example, in atmospheric measurements.

## Experimental Section

The IRPD experiments were carried out using a ring electrode trap and time-of-flight mass spectrometer<sup>[16,17]</sup> temporarily installed at the “Free Electron Laser for Infrared eXperiments” (FELIX) facility<sup>[18]</sup> at the FOM Institute Rijnhuizen (The Netherlands). Gas-phase anions were produced in a commercial Z-spray source from a solution of suberic acid (1 mM) and NaOH (2 mM) in a 20:80 water/acetonitrile mixture. Parent ions were mass-selected in a quadrupole mass filter (Figure S1 in the Supporting Information) and focused into a ring electrode ion trap. To allow for continuous ion loading and ion thermalization, the trap was continuously filled with He gas (ca. 0.01 mbar) at an ion-trap temperature of 15 K. After filling the trap for 99 ms, all ions were extracted from the ion trap and focused both temporally and spatially into the center of the extraction region of an orthogonally mounted linear time-of-flight mass spectrometer. Here, they interacted with the IR laser pulse prior to the application of the extraction voltages. FELIX was operated from 1250–1800  $\text{cm}^{-1}$  with a bandwidth of approximately 0.3% root mean square (RMS) of the central wavelength and average power of 30  $\text{mJ pulse}^{-1}$ . IR spectra were recorded by monitoring all ion intensities simultaneously as the laser wavelength is scanned. The photodissociation cross section  $\sigma$  was determined from the relative abundances of the parent and photofragment ions  $I_0$  and  $I(v)$  and the frequency-dependent laser power  $P(v)$  using  $\sigma = -\ln[I(v)/I_0]/P(v)$ .<sup>[15]</sup>

MD simulations were performed with the CHARMM force field (glutamic acid parameters).<sup>[19]</sup> For successive structure selection and optimization, the SCC-DFTB method,<sup>[20]</sup> DFT (PBE/aug-cc-pVDZ) and CC2/aug-cc-pVDZ were used, the latter two as implemented in turbomole 6.1.<sup>[21]</sup> CEPA/1 (aug-cc-pVDZ basis) calculations were performed with ORCA 2.7.<sup>[22]</sup> Theoretical IR spectra show scaled (factor 1.0246) PBE/aug-cc-pVDZ frequencies. See the Supporting Information for computational details.

Received: October 15, 2010

Published online: March 24, 2011

**Keywords:** carboxylic acids · hydrates · IR spectroscopy · molecular dynamics · solvent effects

- 
- [1] M. Gielen, *Coord. Chem. Rev.* **1996**, *151*, 41–51.
- [2] C. N. R. Rao, S. Natarajan, R. Vaidhyanathan, *Angew. Chem.* **2004**, *116*, 1490–1521; *Angew. Chem. Int. Ed.* **2004**, *43*, 1466–1496.
- [3] D. Grosjean, K. Vancauwenberghe, J. P. Schmid, P. E. Kelley, J. N. Pitts, *Environ. Sci. Technol.* **1978**, *12*, 313–317.
- [4] L. S. Wang, C. F. Ding, X. B. Wang, J. B. Nicholas, B. Nicholas, *Phys. Rev. Lett.* **1998**, *81*, 2667–2670.
- [5] X. B. Wang, L. S. Wang, *Annu. Rev. Phys. Chem.* **2009**, *60*, 105–126.
- [6] X. Yang, Y. J. Fu, X. B. Wang, P. Slavicek, M. Mucha, P. Jungwirth, L. S. Wang, *J. Am. Chem. Soc.* **2004**, *126*, 876–883.
- [7] M. A. Duncan, *Int. J. Mass Spectrom.* **2000**, *200*, 545–569.
- [8] B. Minofar, M. Mucha, P. Jungwirth, X. Yang, Y. J. Fu, X. B. Wang, L. S. Wang, *J. Am. Chem. Soc.* **2004**, *126*, 11691–11698.
- [9] X. B. Wang, J. Yang, L. S. Wang, *J. Phys. Chem. A* **2008**, *112*, 172–175.
- [10] J. M. Weber, J. A. Kelley, S. B. Nielsen, P. Ayotte, M. A. Johnson, *Science* **2000**, *287*, 2461–2463.
- [11] J. Zhou, G. Santambrogio, M. Brummer, D. T. Moore, G. Meijer, D. M. Neumark, K. R. Asmis, *J. Chem. Phys.* **2006**, *125*, 111102.
- [12] M. F. Bush, R. J. Saykally, E. R. Williams, *J. Am. Chem. Soc.* **2007**, *129*, 2220–2221.
- [13] D. J. Goebbert, T. Wende, R. Bergmann, G. Meijer, K. R. Asmis, *J. Phys. Chem. A* **2009**, *113*, 5874–5880.
- [14] S. E. Cabaniss, J. A. Leenheer, I. F. McVey, *Spectrochim. Acta Part A* **1998**, *54*, 449–458.
- [15] J. Oomens, A. G. G. M. Tielens, B. Sartakov, G. von Helden, G. Meijer, *Astrophys. J.* **2003**, *591*, 968–985.
- [16] D. J. Goebbert, G. Meijer, K. R. Asmis, *AIP Conf. Proc.* **2009**, *1104*, 22–29.
- [17] D. J. Goebbert, E. Garand, T. Wende, R. Bergmann, G. Meijer, K. R. Asmis, D. M. Neumark, *J. Phys. Chem. A* **2009**, *113*, 7584–7592.
- [18] D. Oepts, A. F. G. van der Meer, P. W. van Amersfoort, *Infrared Phys. Technol.* **1995**, *36*, 297–308.
- [19] A. D. MacKerell, D. Bashford, M. Bellott, R. L. Dunbrack, J. D. Evanseck, M. J. Field, S. Fischer, J. Gao, H. Guo, S. Ha, D. Joseph-McCarthy, L. Kuchnir, K. Kuczera, F. T. K. Lau, C. Mattos, S. Michnick, T. Ngo, D. T. Nguyen, B. Prodhom, W. E. Reiher Iii, B. Roux, M. Schlenkrich, J. C. Smith, R. Stote, J. Straub, M. Watanabe, J. Wiorkiewicz-Kuczera, D. Yin, M. Karplus, *J. Phys. Chem. B* **1998**, *102*, 3586–3616.
- [20] M. Elstner, D. Porezag, G. Jungnickel, J. Elsner, M. Haugk, T. Frauenheim, S. Suhai, G. Seifert, *Phys. Rev. B* **1998**, *58*, 7260–7268.
- [21] TURBOMOLE V6.1—A development of University of Karlsruhe and Forschungszentrum Karlsruhe GmbH, 1989–2007, available from <http://www.turbomole.com>, TURBOMOLE GmbH, **2009**.
- [22] ORCA—An Ab Initio, DFT and Semiempirical electronic structure package, Version 2.7—Revision 0, Universität Bonn, F. Neese, **2009**.
-